Supporting information for the manuscript

Support Interactions Dictated Active Edge Sites over MoS_2-Carbon Composites for Hydrogen Evolution

*Xiaobin Qiu[a,†], Yewei Huang[a,†], Zhenzhen Nie[a], Beibei Ma[a], Yongwen Tan[b], Zhenjun Wu[*a], Nan Zhang[*b], Xiuqiang Xie[*b]*

[a] *College of Chemistry and Chemical Engineering, Hunan University, Changsha 410082, P. R. China. E-mail: wooawt@hnu.edu.cn.*

[b] *College of Materials Science and Engineering, Hunan University, Changsha 410082, P. R. China. E-mail: nanzhang@hnu.edu.cn; xiuqiang_xie@hnu.edu.cn.*

[†]These authors contribute equally to this work.

Contents list

Figure S1. SEM images of pure MoS_2.

Figure S2. AFM image of MoS_2.

Figure S3. TGA curves of MoS_2/rGO-1, MoS_2/rGO-2, MoS_2/CNT-1 and MoS_2/CNT-2.

Figure S4. TEM images of (a) GO and (b) rGO after MSH treatment. TEM images of CNTs (c) before and (d) after MSH treatment.

Figure S5. SEM images of MoS_2/rGO-2 at different reaction time: (a) 0 min, (b) 2 min, and (c) 4 min.

Figure S6. SEM images of MoS_2/CNT-2 at different reaction time: (a) 0 min, (b) 2 min, and (c) 4 min.

Figure S7. SAED patterns of (a) MoS_2/rGO-2, and (b) MoS_2/CNT-2.

Figure S8. PL spectra of MoS_2/rGO-2 and MoS_2/CNT-2.

Figure S9. Polarization curves of CNT and rGO.

Figure S10. Faradaic efficiency of MoS_2/CNT-2 at 20 mA/cm^2.

Figure S11. Stability test for MoS_2/CNT-2.

Figure S12. XPS spectra of (a) Mo 3d and S 2s peaks, and (b) S 2p peaks of MoS_2/CNT-2 composites before and after HER tests.

Figure S13. Double-layer capacitance analyses for MoS_2. (a) Cyclic voltammograms in the region of 0.1–0.4 V vs. RHE at different scan rates. (b) The plots of current densities against scan rates. Δj is the difference between anodic and cathodic current densities at 0.23 V vs. RHE. The same parameters are used for the tests below.

Figure S14. Double-layer capacitance analyses for MoS_2/rGO-1.

Figure S15. Double-layer capacitance analyses for MoS_2/rGO-2.

Figure S16. Double-layer capacitance analyses for MoS_2/CNT-1.

Figure S17. Double-layer capacitance analyses for MoS_2/CNT-2.

Figure S18. Nitrogen adsorption-desorption isotherms of (a) MoS_2, (b) MoS_2/rGO-1, (c) MoS_2/rGO-2, (d) MoS_2/CNT-1, and (e) MoS_2/CNT-2. (f) BET surface areas of MoS_2, MoS_2/rGO-1, MoS_2/rGO-2, MoS_2/CNT-1 and MoS_2/CNT-2 based on nitrogen adsorption-desorption isotherms.

Figure S19. Polarization curves of MoS_2/CNT-3 and MoS_2/CNT-4.

Table S1 Representative top-down strategies to prepare 2D MoS_2.

Table S2 Comparison of some representative bottom-up strategies recently reported to prepare MoS_2.

Table S3 C 1s XPS results of GO and CNTs.

Table S4 Electrocatalytic performances comparison of our MoS_2-carbon composites with recent related literatures.

References

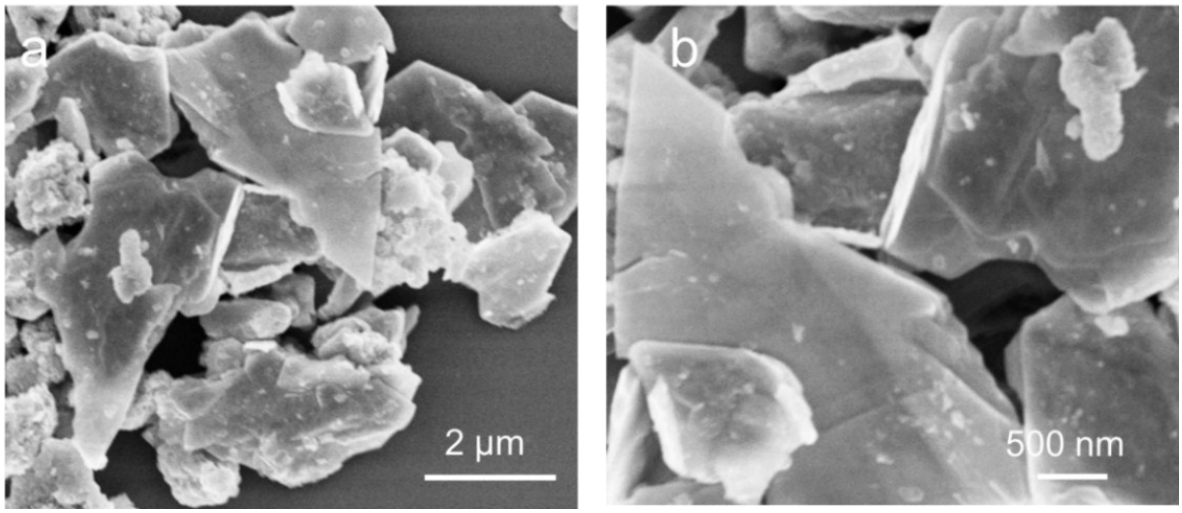

Figure S1. SEM images of pure MoS_2.

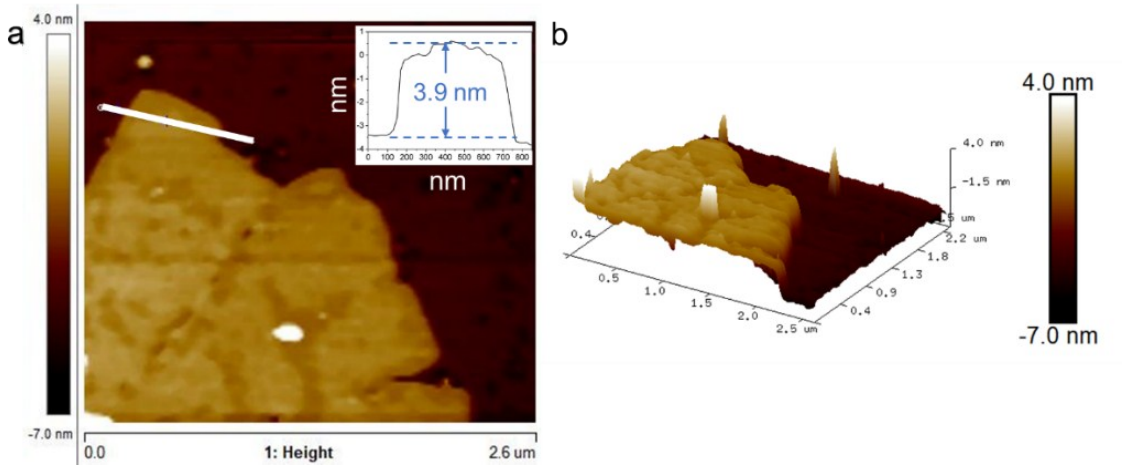

Figure S2. AFM image of MoS_2.

From the AFM results **(Fig. S2)**, the pure MoS_2 has a thickness of 3.9 nm, which is roughly the thickness of 6 layers of MoS_2.

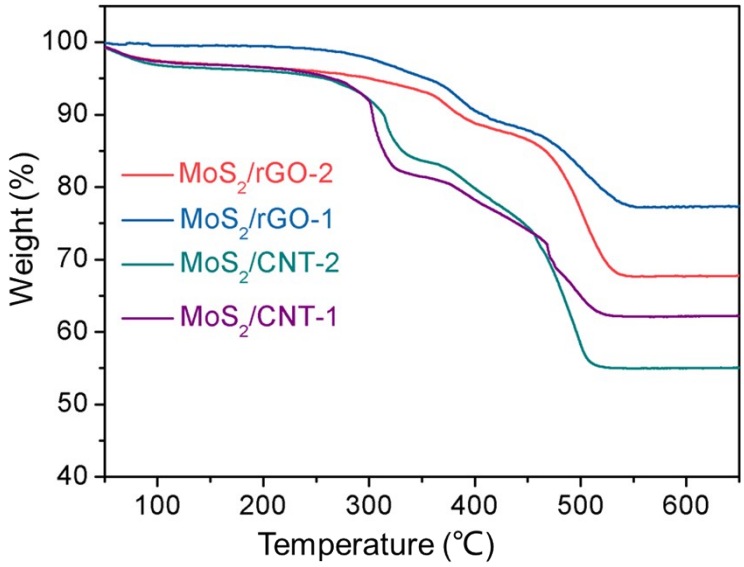

Figure S3. TGA curves of MoS_2, MoS_2/rGO-1, MoS_2/rGO-2, MoS_2/CNT-1 and MoS_2/CNT-2.

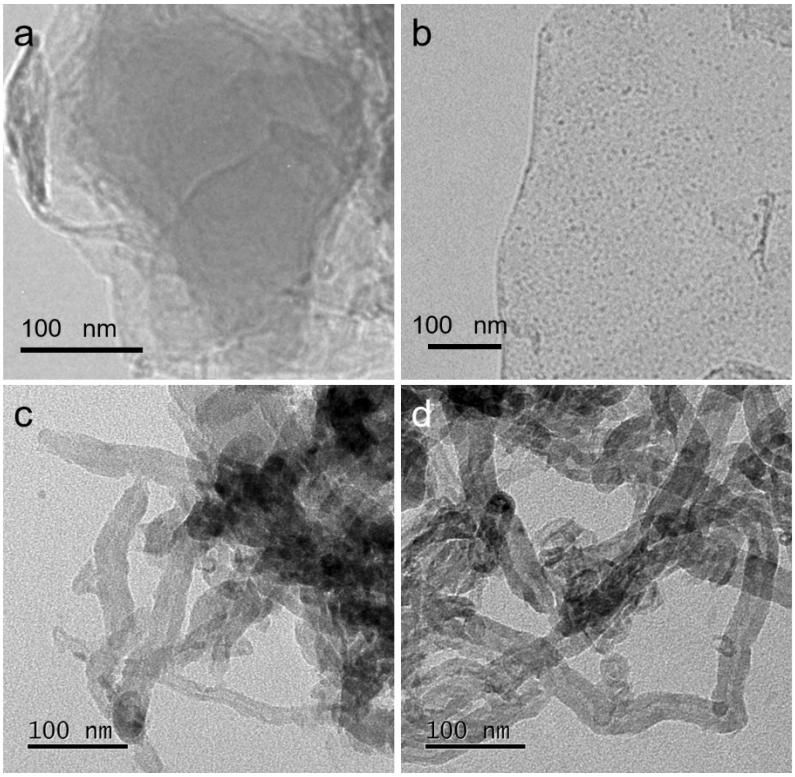

Figure S4. TEM images of (a) GO and (b) rGO after MSH treatment. TEM images of CNTs (c) before and (d) after MSH treatment.

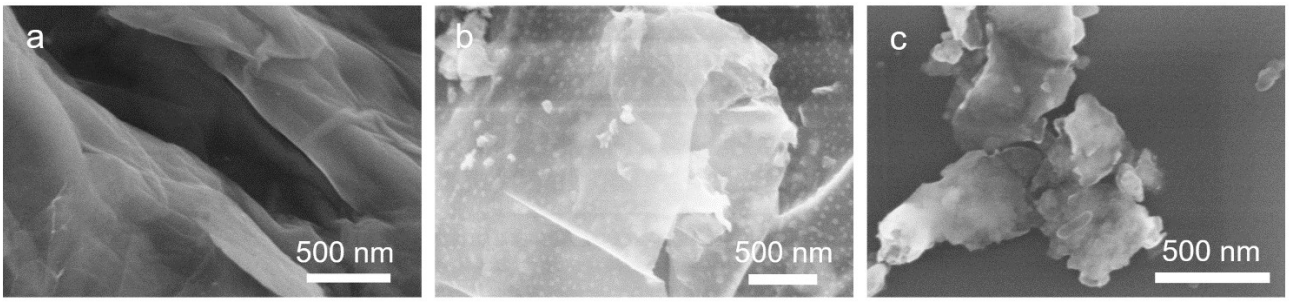

Figure S5. SEM images of MoS_2/rGO-2 at different reaction time: (a) 0 min, (b) 2 min, and (c) 4 min.

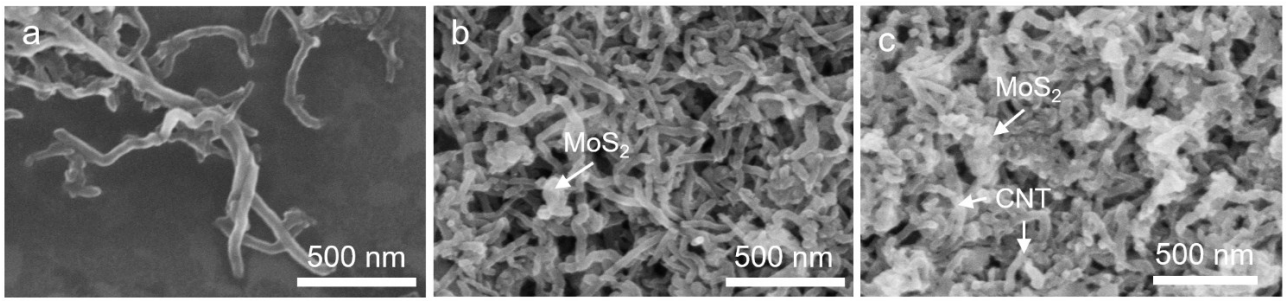

Figure S6. SEM images of MoS_2/CNT-2 at different reaction time: (a) 0 min, (b) 2 min, and (c) 4 min.

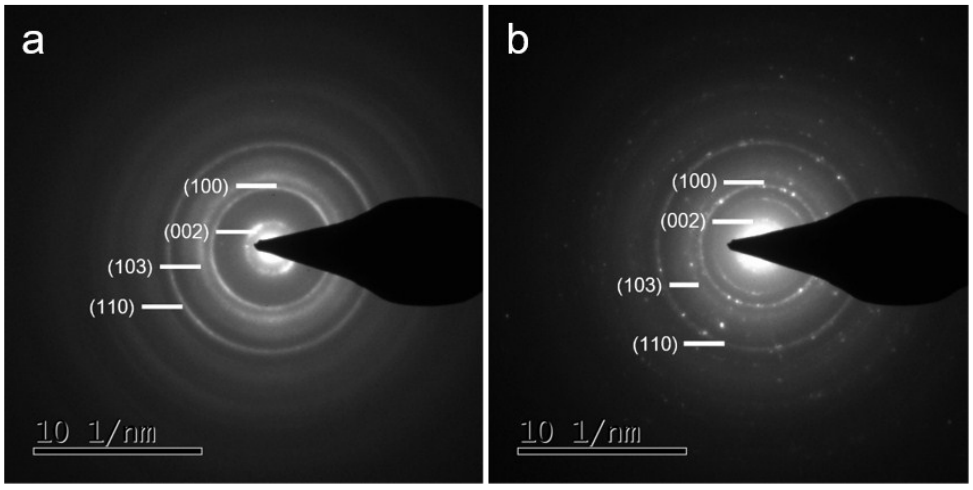

Figure S7. SAED patterns of (a) MoS_2/rGO-2, and (b) MoS_2/CNT-2.

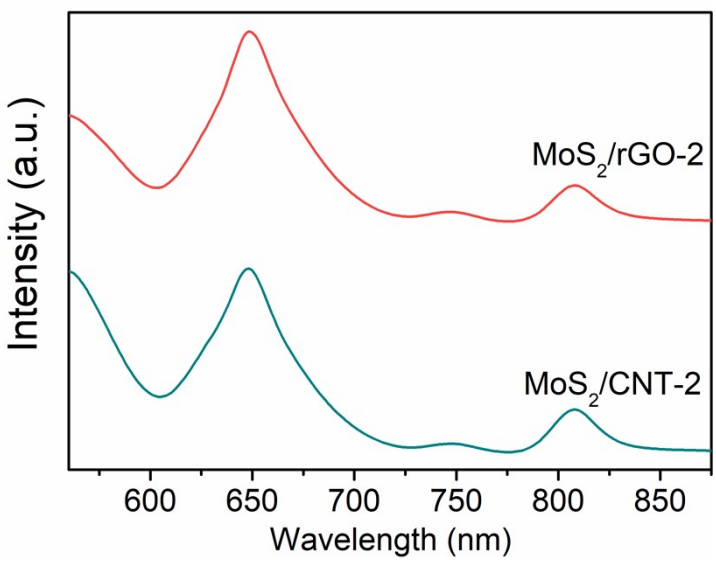

Figure S8. PL spectra of MoS_2/rGO-2 and MoS_2/CNT-2.

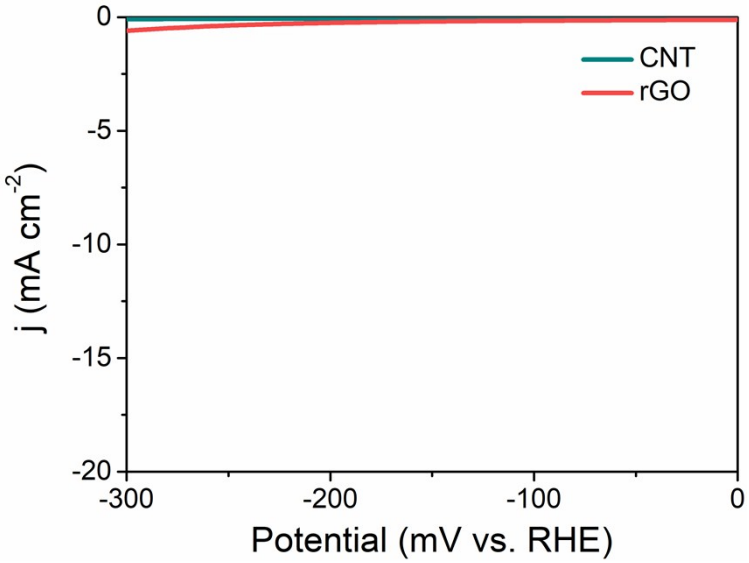

Figure S9. Polarization curves of CNT and rGO.

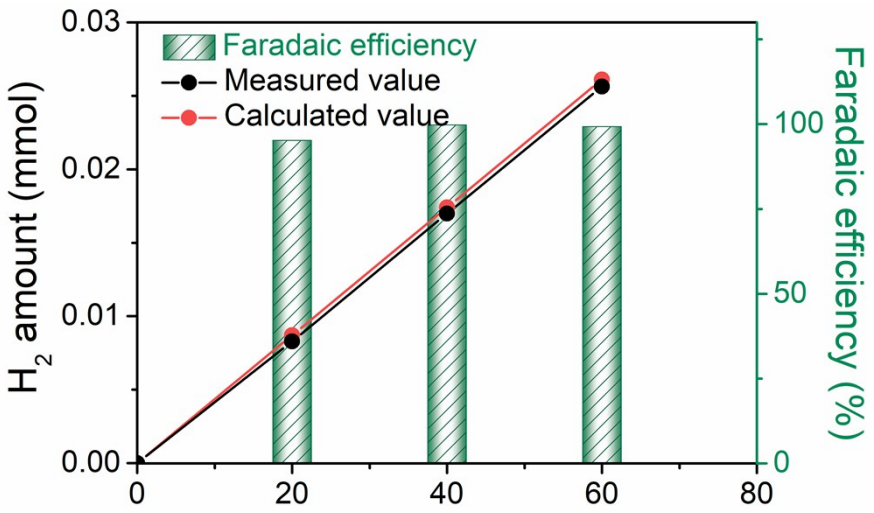

Figure S10. Faradaic efficiency of MoS_2/CNT-2 at 20 mA/cm^2.

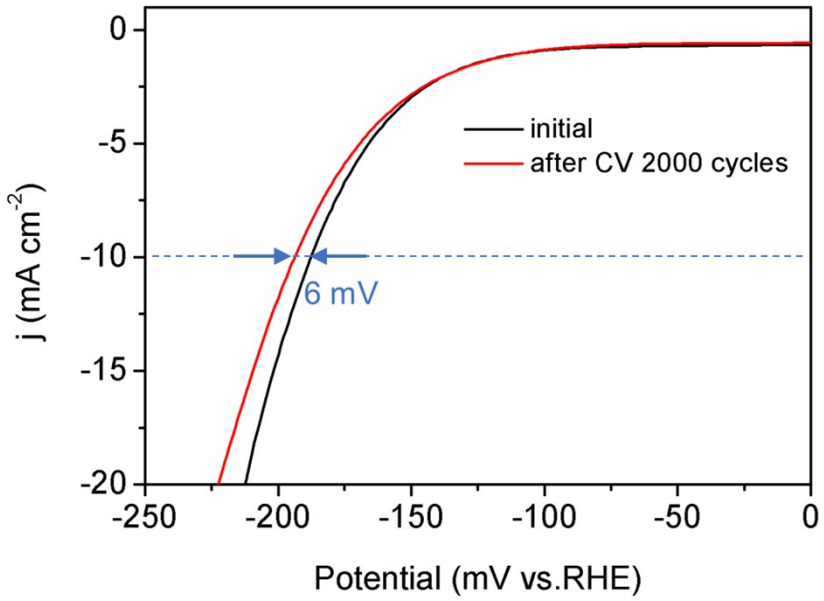

Figure S11. Stability test for MoS_2/CNT-2.

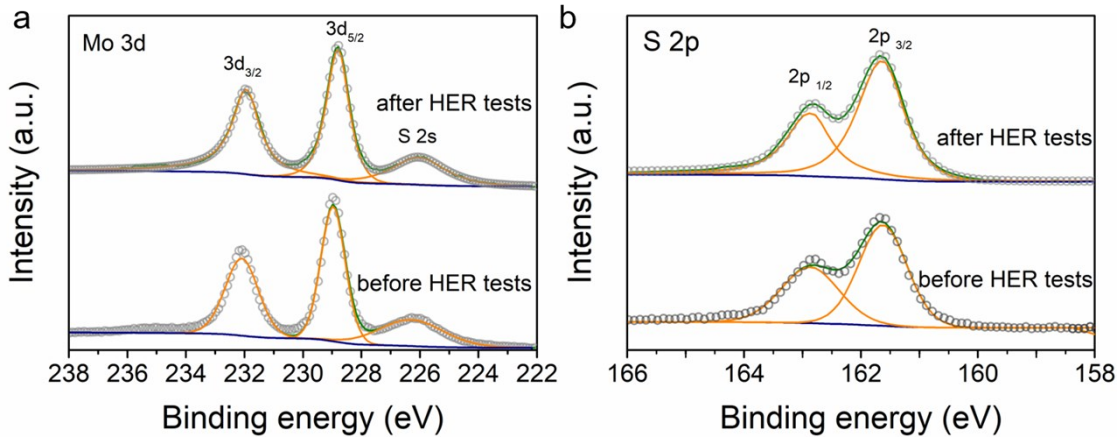

Figure S12. XPS spectra of (a) Mo 3d and S 2s peaks, and (b) S 2p peaks of MoS_2/CNT-2 composites before and after HER tests.

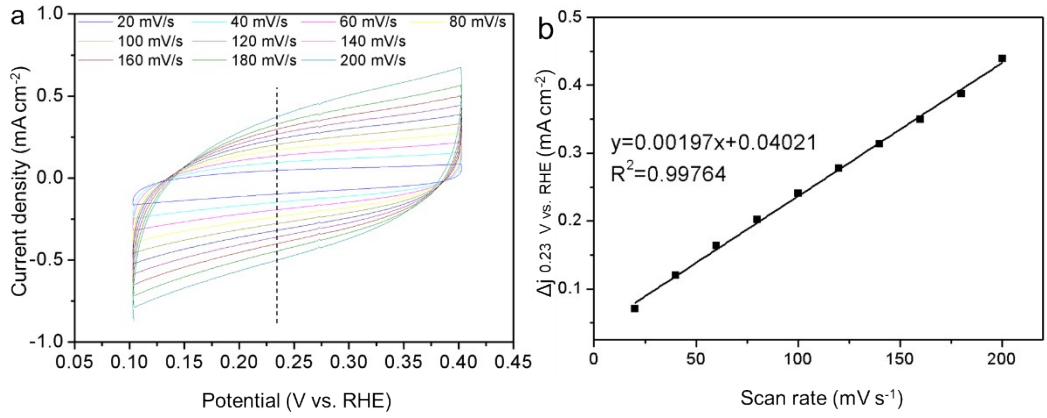

Figure S13. Double-layer capacitance analyses for MoS_2. (a) Cyclic voltammograms in the region of 0.1–0.4 V vs. RHE at different scan rates. (b) The plots of current densities against scan rates. Δj is the difference between anodic and cathodic current densities at 0.23 V vs. RHE. The same parameters are used for the tests below.

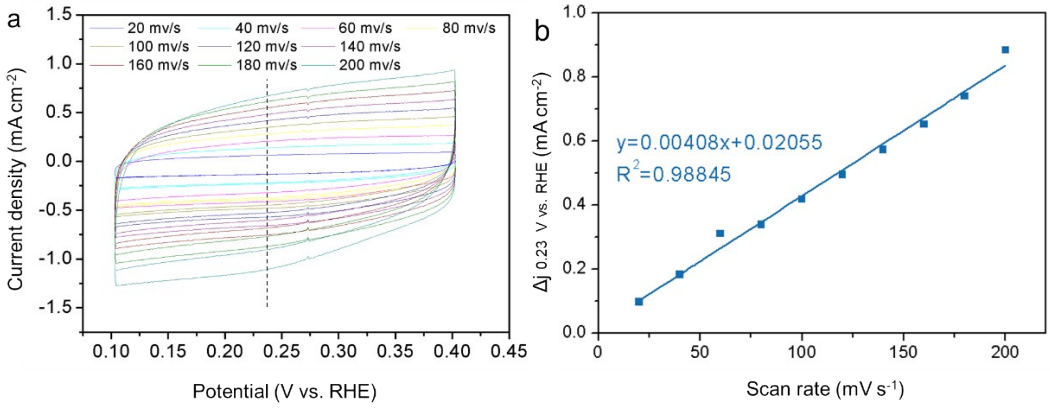

Figure S14. Double-layer capacitance analyses for MoS_2/rGO-1.

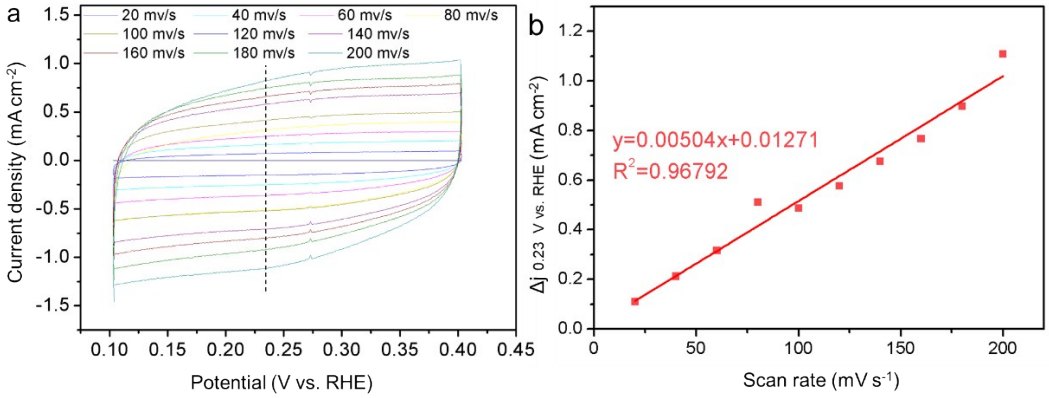

Figure 15. Double-layer capacitance analyses for MoS_2/rGO-2.

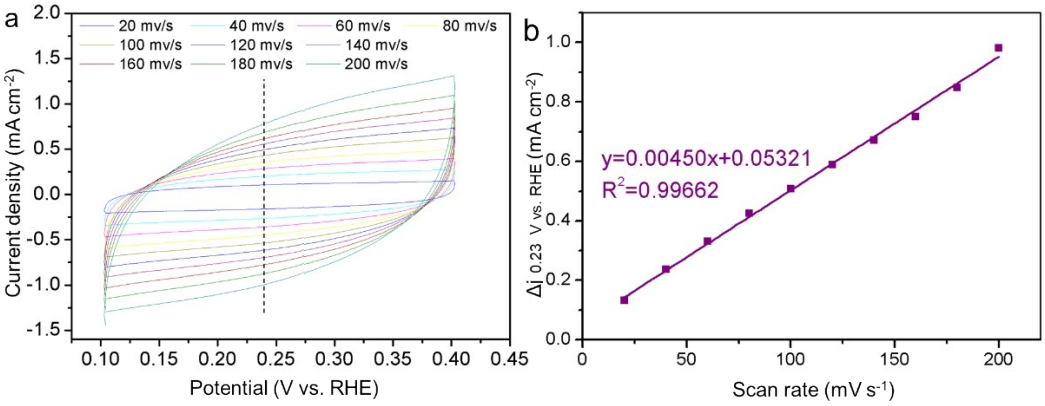

Figure S16. Double-layer capacitance analyses for MoS_2/CNT-1.

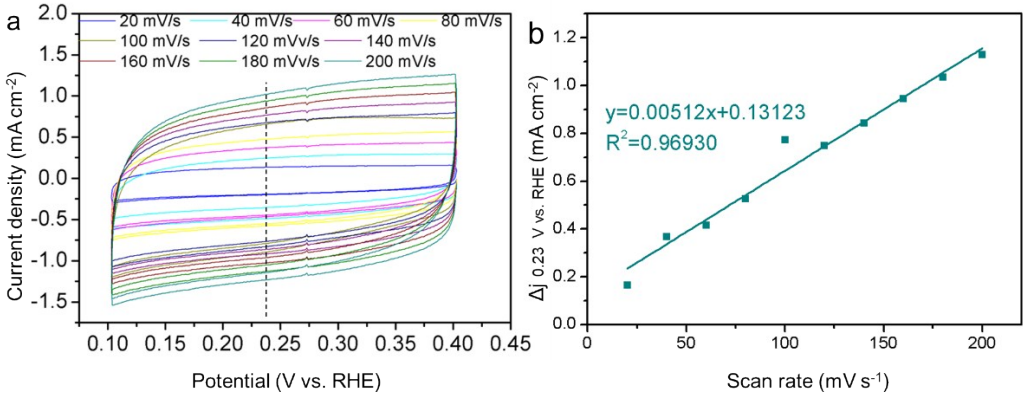

Figure S17. Double-layer capacitance analyses for MoS_2/CNT-2.

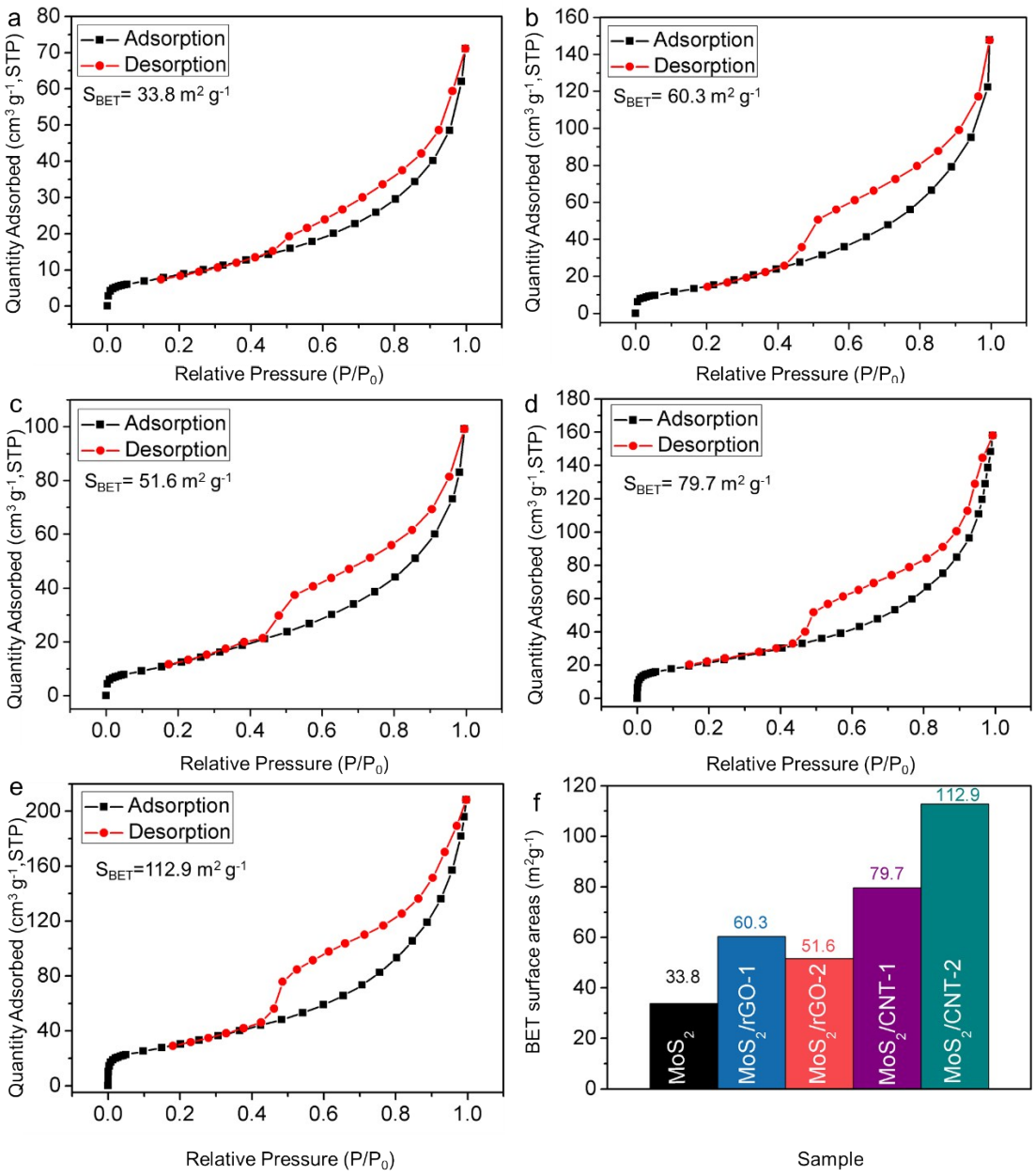

Figure S18. Nitrogen adsorption-desorption isotherms of (a) MoS_2, (b) MoS_2/rGO-1, (c) MoS_2/rGO-2, (d) MoS_2/CNT-1, and (e) MoS_2/CNT-2. (f) BET surface areas of MoS_2, MoS_2/rGO-1, MoS_2/rGO-2, MoS_2/CNT-1 and MoS_2/CNT-2 based on nitrogen adsorption-desorption isotherms.

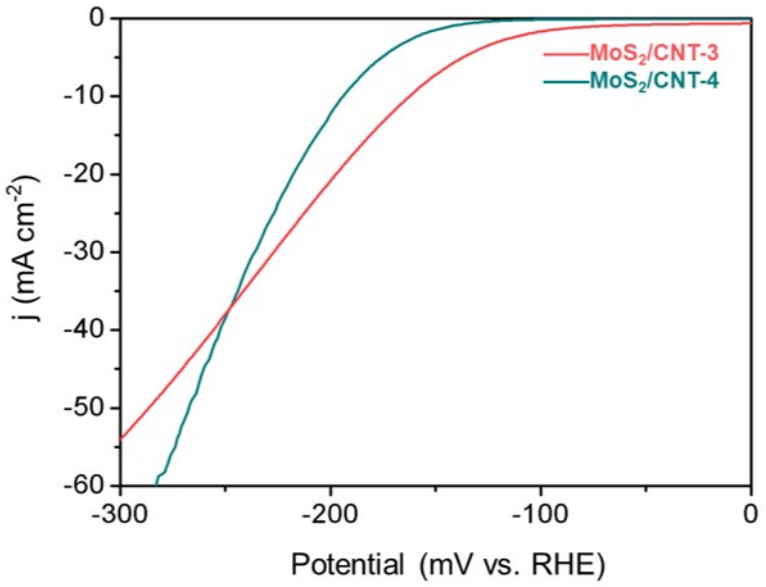

Figure S19. Polarization curves of MoS_2/CNT-3 and MoS_2/CNT-4.

As shown in **Fig. S19**, when the amount of CNTs was increased to 75 mg, the resulting products (denoted as MoS_2/CNT-3) exhibit an overpotential of 163 mV. A further increase of the CNTs feeding amount to 100 mg generates MoS_2/CNT-4, which has an increased overpotential of 195 mV compared to that of MoS_2/CNT-3.

Table S1 Representative top-down strategies to prepare 2D MoS_2.

Reagent	Time (h)	Yield (%)	Ref.
Cetyltrimethylammonium bromide/sodium dodecyl sulfate	8	N/A	1
Polyvinylpyrrolidone	9	N/A	2
Dimethylformamide	1	N/A	3
Dimethylformamide	6	2.5~3	4
Methyllithium/n-butyllithium/tert-butyllithium	72	N/A	5
Chitosan	1	3.7	6

Table S2 Comparison of some representative bottom-up strategies recently reported to prepare MoS_2.

Molybdenum source	Sulfur source	Medium	Time	Temp. (°C)	Ref.
Sodium molybdate	Thiourea	Ethanol	24 h	180	7
Molybdenum trioxide	Thioacetamide	Ethanol	18 h	200	8
Sodium molybdate	L-cysteine	Ethanol, water	24 h	220	9
Hexacarbonylmolybdenum	Sulfur	Acetone	8 h	180	10
Ammonium tetrathiomolybdate	Ammonium tetrathiomolybdate	Water	24 h	200	11
Sodium molybdate	Thiourea	Water	12 h	200	12
Ammonium molybdate	Thiourea	Water	24 h	200	13
Molybdenum trioxide	Potassium thiocyanate	Water	24 h	210	14
Sodium molybdate	Thioacetamide	Water	24 h	220	15
Sodium molybdate	Thiourea	Steam	5 min	N/A	This work

Table S3 C 1s XPS results of GO and CNTs.

Sample	C=C and C-C (at.%)	C-O (at.%)	C=O (at.%)
Pristine GO	43.1	37.5	19.4
GO after MSH treatment	62.4	24.3	13.3
Acid treated CNTs	38.8	48.6	12.6
CNTs after MSH treatment	45.9	38.6	10.5

Table S4 Electrocatalytic performances comparison of our MoS_2-carbon composites with recent related literatures.

Substrate	MoS_2 ratio (wt%)	Overpotential (mV)	Tafel slope (mV/dec)	C_{dl} (mF/cm^2)	Ref.
Graphene	70	132	45	32.73	16
Graphene	~ 44	~ 150	41	N/A	17
rGO	82.8	156	44	~ 65.6	18
Nitrogen-doped graphene	N/A	208	79	28.1	19
Sulfur-doped graphene	25	290	152	N/A	20
Graphene	22.3	~ 560	61	N/A	21
Oxidized CNT	N/A	~ 200	47	31	22
Nitrogen-doped CNTs on carbon paper	N/A	160	36	N/A	23
Acid-treated CNTs	N/A	~ 184	44.6	N/A	24
rGO	86.1	216	56.66	4.08	MoS_2/rGO-1, this work
rGO	75.3	218	56.76	5.04	MoS_2/rGO-2, this work
CNTs	69.2	225	72.99	4.50	MoS_2/CNT-1, this work
CNTs	49.6	194	52.70	5.12	MoS_2/CNT-2, this work
[a]CNTs	-	163	N/A	N/A	MoS_2/CNT-3, this work

Note: [a]The feeding amount of CNTs is increased to 75 mg, and other experimental procedures are identical to that of MoS_2/CNT-1 and MoS_2/CNT-2. The overpotential is that at j = - 10 mA/cm^2.

References

1. A. Gupta, V. Arunachalam and S. Vasudevan, *J. Phys. Chem. Lett.*, 2015, **6**, 739-744.
2. J. Liu, Z. Zeng, X. Cao, G. Lu, L.-H. Wang, Q.-L. Fan, W. Huang and H. Zhang, *Small*, 2012, **8**, 3517-3522.
3. Q. D. Truong, M. Kempaiah Devaraju, Y. Nakayasu, N. Tamura, Y. Sasaki, T. Tomai and I. Honma, *ACS Omega*, 2017, **2**, 2360-2367.
4. C. Wang, D. Ren, H. S. Park, Z. Dong, Y. Yang, Q. Ren and X. Yu, *J. Alloys Compd.*, 2017, **728**, 767-772.
5. A. Ambrosi, Z. Sofer and M. Pumera, *Small*, 2015, **11**, 605-612.
6. S. Guo, Z. Qian, Z. Zhu, J. Xie, J. Fan, Q. Xu, P. Shi and Y. Min, *ChemistrySelect*, 2017, **2**, 3117-3128.
7. J. Wang, X. Zhao, Y. Fu and W. Xin, *Appl. Surf. Sci.*, 2016, **399**, 237-244.
8. X. Geng, Y. Jiao, H. Yang, A. Mukhopadhyay, Y. Lei and H. Zhu, *Adv. Funct. Mater.*, 2017, **27**.
9. Q. Pang, Y. Zhao, X. Bian, Y. Ju, X. Wang, Y. Wei, B. Liu, F. Du, C. Wang and G. Chen, *J. Mater. Chem. A*, 2017, **5**, 3667-3674.
10. L. Nan, Z. Liu, G. Qian, X. Li, R. Wang, Y. Xiao and Y. Li, *J. Mater. Sci.*, 2017, **52**, 13183-13191.
11. Z. Li, A. Ottmann, T. Zhang, Q. Sun, H. P. Meyer, Y. Vaynzof, J. Xiang and R. Klingeler, *J. Mater. Chem. A*, 2017, **5**.
12. Y. Jiang, Y. Guo, W. Lu, Z. Feng, B. Xi, S. Kai, J. Zhang, J. Feng and S. Xiong, *ACS Appl. Mater. Interfaces*, 2017, **9**, 27697-27706.
13. C. Li, J. Li, Z. Wang, S. Zhang, G. Wei, J. Zhang, H. Wang and C. An, *Inorg. Chem. Front.*, 2017, **4**, 309-314.
14. S. Liang, Z. Jiang, L. Jing, A. Pan, T. Yan, C. Tao and G. Fang, *Crystengcomm*, 2013, **15**, 4998-5002.
15. H. Lin, X. Chen, H. Li, M. Yang and Y. Qi, *Mater. Lett.*, 2010, **64**, 1748-1750.
16. Y. Li, B. He, X. Liu, X. Hu, J. Huang, S. Ye, Z. Shu, Y. Wang and Z. Li, *Int. J. Hydrogen Energy*, 2019, **44**, 8070-8078.
17. Y. Li, H. Wang, L. Xie, Y. Liang, G. Hong and H. Dai, *J. Am. Chem. Soc.*, 2011, **133**, 7296-7299.
18. S. Khazraei, M. Karimipour, M. Molaei and M. R. Moghadam, *Int. J. Hydrogen Energy*, 2019, **44**, 13284-13295.
19. D. M. Nguyen, P. D. Hai Anh, L. G. Bach and Q. B. Bui, *Mater. Res. Bull.*, 2019, **115**, 201-210.
20. A. Kagkoura, M. Pelaez-Fernandez, R. Arenal and N. Tagmatarchis, *Nanoscale Adv.*, 2019, **1**, 1489-1496.
21. L. Xu, Y. Gu, Y. Li, H. Liu, Y. Shang, Y. Zhu, B. Zhou, L. Zhu and X. Jiang, *J. Colloid Interface Sci.*, 2019, **542**, 355-362.
22. H. Huang, W. Huang, Z. Yang, J. Huang, J. Lin, W. Liu and Y. Liu, *J. Mater. Chem. A*, 2017, **5**, 1558-1566.
23. J. Ekspong, T. Sharifi, A. Shchukarev, A. Klechikov, T. Wågberg and E. Gracia-Espino, *Adv. Funct. Mater.*, 2016, **26**, 6766-6776.
24. Y. Yan, X. Ge, Z. Liu, J.-Y. Wang, J.-M. Lee and X. Wang, *Nanoscale*, 2013, **5**, 7768-7771.